

平成 24 年度

三重大学大学院 生物資源学研究科

修士論文

**Impact of the winter North Atlantic Oscillation
on the Western Pacific region in the following winter**

冬季北大西洋振動が翌冬の西太平洋域の天候に及ぼす影響

Climate and Ecosystems Dynamics Division

Graduate school of Bioresources

Mie University

Miki Oshika

Supervisor: Yoshihiro Tachibana

26 February 2013

Abstract

Using 51-year reanalysis data, we propose that the winter Western Pacific (WP) pattern, which brings about a warm and cold winter in Japan, is associated with the previous winter North Atlantic Oscillation (NAO). We focus on the Arctic sea-ice fluctuation and El Niño/Southern Oscillation (ENSO) related to the weather in Japan about the mechanism regarding the relationship of the winter WP with the winter NAO in the previous year. We calculate the lag correlation of the geopotential height, the sea-ice and the Sea Surface Temperature (SST) with the winter WP index which divided into the low, middle and high frequency variations. The negative (positive) phase of the winter WP associates with the positive (negative) phase of the previous winter NAO. The positive (negative) phase of the low-frequency winter NAO variation impacts the sea-ice decrease (increase) in spring and summer while the middle-frequency NAO variation impacts the La Niña (El Niño) phenomenon in winter from summer. We suggest the winter NAO is a candidate for exciting the winter WP in the following winter through both the sea-ice and the ENSO.

1. Introduction

The persisting cold wave and the heavy snowfall in the wintertime East Asia have a social, economic and psychological impact on Japan because of the lack of atomic power station in the era of post-Fukushima accident. The colder winter is the more electricity is needed. The cold wave and heavy snowfall are associated with the hemispheric anomalous atmospheric circulations. For example, the Western Pacific (WP) and Eurasian (EU) patterns, which are well-known teleconnection patterns defined by Wallace and Gutzler [1981], have an impact on the anomalous atmospheric circulation in the East Asia. It is thus important to find out the formation process of the WP pattern, which has a significant influence on society, and so on.) Whether the WP pattern in coming winter is anomalous or not is important for not only the scientists but also the Japanese who are worry about the lack of the electricity. Thus, the long-term forecast for the wintertime WP pattern is important.

Honda et al (2009) hypothesized that wintertime weather in the East Asia is related to the ice reduction of the Barents Kara Sea in the previous autumn. Their AGCM results indicate that the decrease of the sea-ice in summer and autumn strengthens the Siberian anticyclone, and brings about cold anomaly in East Asia. Although they did not directly note the WP pattern, the ice reduction in the autumn may give us the key to the long-term forecast in the winter in the East Asia. In fact, some figures in their reanalysis data look similar to the WP. Also, Takano et al (2008) showed that Siberian-Japan pattern, which is similar to the WP pattern, is favorable for the heavy snowfall in Japan. Hori et al (2011) also pointed that arrival of the cold wave to East Asia is related to the anticyclonic anomaly formed in association with the sea ice decline of the Barents-Kara Sea.

Ogi et al (2003) showed that summertime sea ice over the Barents Sea and summertime weather in the East Asia are related to the wintertime North Atlantic Oscillation (NAO) in the previous year. The impact of the NAO in the Arctic Sea ice along with the Barents Sea is also pointed out by Rodwell et al (1999). The some kinds of previous studies introduced above, suggest that the winter cold wave in East Asia should potentially be associated with the previous winter

NAO. However, no previous studies have been examined the predictability of the winter WP pattern from the NAO in the previous winter. The first purpose of the present study is to confirm that the winter WP pattern has an association with the previous winter NAO.

El Niño/Southern Oscillation (ENSO) is well-known another key factor for long-term prediction. WP pattern is known as one of the most dominant teleconnection patterns that are excited by ENSO [e.g., Horel and Wallace, 1981; Mo and Livezey, 1986; Kodera 1998]. For example, Horel and Wallace (1981) showed that the winter El Niño events and the negative phase of the Southern Oscillation Index (SOI) are associated with the positive phase of the winter WP.

Therefore, the influence of both the tropics, e.g., ENSO and the Arctic, e.g., the sea-ice should be considered. As the previous studies suggested, the winter WP pattern can be related to both the NAO and ENSO. If interannual variation of the NAO is has some relationship with ENSO, the linkage mechanism among the WP, NAO, and ENSO would be complicated. For example, if NAO influence the ENSO, or if ENSO influences the NAO, careful consideration should be took into account. For example, Nakamura et al (2006, 2007) demonstrated that springtime AO influences the ENSO in the following winter. Because Arctic Oscillation (AO) and NAO have similar structure in the Atlantic northern hemisphere, NAO might also have some influences on the ENSO. The second purpose of the present study is to distinguish the cause and effect of the three; NAO, WP and ENSO. In particular, a possible the influence of the NAO on the ENSO is demonstrated. Finally, the formation process of the WP pattern from both low and high latitudes are discussed. The method of this study is mainly by statistical analyses using reanalysis data set for the period of about a half century.

2. Data and Method

The atmospheric data used in this study is the National Centers for Environmental Prediction and National Centers for Atmospheric Research (NCEP/NCAR) reanalysis data [Kalnay et al., 1996]. The sea-ice concentration and the sea surface temperature (SST) data used in this study is a Met Office Hadley Center's sea ice and sea surface temperature data set version 1 (HadISST1) [Rayner et al., 2003]. The ground snow depth data from 1979 through 2010 by the JMA Climate Data Assimilation System reanalysis (JCDAS) is also used in this study. We used monthly mean data from 1960 to 2010 except of the snow data. We defined that the winter WP index is the time series of the first leading mode by an Empirical Orthogonal Function (EOF) Analysis of the monthly mean 500hPa geopotential height in December over the Pacific sector, 20°-80°N, 120°-180°E.

To examine the existence of relationship between the winter WP and the previous winter NAO, we calculate the lag correlation of the previous winter atmospheric fields with the winter WP index. As details are shown in the following sections, a significant relation between the WP and the NAO in the previous winter was found. To assess the relationship between the winter WP and the previous winter NAO objectively, we apply a coupled EOF analysis by using geopotential height data of Western Pacific covering the WP area in a winter and those of North Atlantic covering NAO area in the winter one year before. Here, the NAO area is over the Atlantic sector, 30°-90°N, 50°W-10°E, and the WP area is the same as the WP index. As details are shown in the following sections, a coupled NAO and WP pattern was found in the leading mode of the coupled EOF. We define the time series of the leading mode of the coupled EOF as the NAO+WP index. To find out the linking process of the winter WP in the next year, we calculate the seasonal evolution of the linearly regressed sea-ice, SST fields with the winter NAO+WP index. The time series of the NAO+WP index are divided into low, middle and high frequency variations. The low frequency data defined in this study is 7-year running mean. The high frequency data is original data minus 3-year running mean. The middle data is the band pass filtered data that is the original data minus

7-year running mean and minus the high frequency data. In this analysis, we have removed linear trend from the sea-ice concentration of each grid point before calculating the lag correlation of the Arctic sea-ice with the NAO+WP index, because the strong decrease trend of the sea ice might hide significant relationship.

3. Results

3.1. The winter WP and the previous winter NAO

Figure 1a shows the simultaneous spatial correlation of the first leading mode from the EOF analysis of the geopotential height at 500hPa over the Pacific sector, 20°-80°N, 120°-180°E. A significant north-south dipole pattern is seen over the western part of the North Pacific; the high is over Japan whereas low over Russian Far East. The contribution of the first mode is 39.8% and second mode is 22.6%. The pattern is quite similar to that of the original WP pattern first defined by Wallace and Gutzler (1981), in which two points correlation was applied. Figure 1a-2 shows simultaneous correlated temperature map at 1000hPa with the WP index. The temperature over Japan is anomalously high and Russian Far East is anomalously low. It therefore is confirmed that the WP pattern is the most amplified pattern around Japan in winter, and its influence on the weather Japan is the most dominant. The positive of the WP index defined in this study is cold north and warm south. Since the negative WP is in reversed phase of the pattern, Japan is overall cold winter in the negative WP index.

Figure 2 shows the lag correlation map of the geopotential height at 500-hPa in December of the previous year with the winter WP index of the EOF analysis. The significantly positive correlation in the Iceland and negative correlation in the North Atlantic Ocean are shown in Figure 2. This geopotential height anomaly is quite similar to the negative phase of the NAO pattern defined by Wallace and Gutzler (1981). This lagged significant correlation indicates that when the winter NAO is negative (positive) phase, the positive (negative) phase of the WP pattern appears and the warm (cold) anomaly is tends to be brought in the Far East in the following winter. To assess this one-year-lag relationship objectively, we performed the EOF analysis by using the data coupling the areas covering the action center of the NAO in December and the WP in the following December. The first mode of this coupled EOF analysis is shown in Figure 3. The contribution of the first mode is 29.7% and second mode is 16.5%. The successive occurrence of the negative phase of the NAO and the positive phase of the WP in the following winter is the most dominant. The

same one-year-lag connection as shown in Figure 2 was demonstrated in this EOF analysis, and we define this first leading mode index as NAO+WP index.

3.2. The process from the winter NAO to the following winter WP

In order to account for the connection of the NAO and WP pattern in the next year, the memory that is not in the atmosphere is needed because the atmosphere itself does not have such a large memory that influences the phenomena in the next year. Some candidates are the ocean, land, and sea ice since their heat capacity is much larger than that of the atmosphere. Here we demonstrate some oceanic processes playing roles in connecting these two atmospheric patterns. Figure 4 shows the correlation of the Arctic sea-ice concentration in spring (left), summer (middle) and autumn (right) with the winter NAO+WP index. There are the positive correlations in the Eurasian side of the Arctic Sea, in particular Barents Sea, in spring, summer and autumn with the winter NAO+WP index. This means that the linkage of the previous winter positive (negative) NAO and negative (positive) WP with cold Japan in the following winter is in association with the decrease (increase) of sea-ice in the Arctic in spring through autumn. The correlation coefficients with the long-term moving averaged data are large as compared to those with short-term moving average. There were no correlation between the high-frequency or band-passed NAO+WP index and sea-ice in the Arctic sea (Figures not shown). The correlation pattern of the Arctic sea ice with the WP index with low pass filter were also almost the same as in Figure 4 (Figure not shown). These results suggest that long-term variation of the summertime sea-ice is a key to connecting the two winter teleconnection patterns.

The sea-ice decrease of the Barents Sea in spring and summer connection with the winter negative NAO and the following winter positive WP is consistent with the result of the influenced by the winter NAO of Ogi *et al.* (2003). Further, the relationship that the decrease of the Arctic sea-ice cover in the summer brings the cold anomaly in the Far East in the winter is consistent with the result of Honda *et al.* (2009).

Other oceans may have an important role in the linkage of the NAO and WP. Figure 5 shows the global-scale correlation map of the SST with the winter NAP+WP index. ENSO signal is obvious. This indicates that El Niño and WP simultaneously tend to occur after one year of the negative phase of the winter NAO. Next, we demonstrate the time evolution of El Niño-South Oscillation (ENSO). Figure 6 shows the time-longitude cross section of the longitudinal averaged SST at 10°S-10°N of the correlated with the winter NAO+WP index filtered by three high-pass (a) less than 3 years, (b) less than 5 years, (c) less than 7 years and (d) band-pass between 3-7years. There are the positive correlations in the central and eastern Pacific Ocean from summer to winter except of the 3years high-pass filtered data. In addition, the correlation of the band-pass between 3-7years is the highest. This SST correlation area is in accordance with the positive SST anomaly area when El Niño develops. In contrast, the low-pass filtered SST does not have any significant correlations in the tropics with the winter NAO+WP index (Figures not shown). Not the decadal ENSO or quasi-biennial oscillation (QBO) time scales but the time scale involved in the ENSO does associate with the NAO and WP linkage. Similar SST developing signature correlated with the previous winter NAO index with band pass filtered was also seen in the tropical Pacific (Figure not shown). In summary, if winter NAO is negative (positive) phase, then El Niño (La Niña) develops from summer to winter, and warm (cold) winter brings about Japan in association with positive (negative) WP.

To estimate the strength of this relationship among three phenomena; NAO in the previous winter, ENSO and WP, we execute an EOF analysis by using three kinds of the data; the 500hPa geopotential height data in the area of the NAO in December, and those of the WP in the following December, and the SST in the ENSO area in the following December. Here, the ENSO area is over the Pacific sector, 10°S-10°N, 90°W-180°W, and the NAO and the WP area is same as those of the NAO+WP index. The EOF is calculated by using the standardized data, i.e., by using correlation matrix. Because EOF analysis data is weighted in the latitude direction, we set that the areas of the NAO, the WP and the ENSO are almost equal size. Figure 7 shows the horizontal pattern of the first

mode of the EOF. The EOF pattern signifies the occurrence of the negative phase of the NAO, the positive phase of the WP and El Niño. The same relationship was seen in this EOF analysis, and we defined the time series of this leading mode as the NAO+WP+ENSO index. The contribution of the first mode is 31.7% and the second mode is 13.5%. We can also confirm that the NAO, WP and ENSO are closely tied with each other.

4. Discussion

We indicated that the winter NAO has the potential to be associated with the following winter WP, and bring the temperature anomaly in the Far East. In addition, we called for that there are two processes of the low and high latitude influences with the relationship between the wintertime NAO and the following winter WP. The first of these is the low-frequency variation of the Arctic sea-ice in spring trough autumn and the second is the high-frequency ENSO from summer to winter. Thus, the low and high frequency NAO act on sea-ice and SST through a different process, and excite WP in the following winter. Furthermore, we supported the relationship between NAO and WP by defining the NAO+WP index, which set up from EOF analysis with the data coupling the both area of the winter NAO and the following winter WP. In the same way, we evaluate relationship of the NAO, the ENSO and the WP objectively by use of the NAO+WP+ENSO index. In the process from the winter NAO to the summer ENSO, we suggested that the snow anomaly in the western Eurasian Continent by the influence of the winter NAO, by the association of some following articles.

Clark et al., (1999) and Hori and Yasunari, (2003) showed that the winter NAO impacts on the snow in the western Eurasia Continent, and Barnett et al., (1989) showed that the winter snow in the Eurasia Continent is associated with the summer Indian monsoon and ENSO each other. In addition, Nakamura et al., (2006, 2007) showed that the cold air outbreak from Asia to the tropical zone intensifies the western burst on the western tropical Pacific and becomes the trigger of El Niño. Thus, the winter NAO has possibilities to intensify the cold air outbreak by the snow anomaly in the western Eurasia Continent. We can therefore hypothesize that tropical atmosphere and ocean respond by the snow anomaly associated with the wintertime NAO, and then El Niño outbreaks. To examine this hypothesis, we examine Eurasian snow anomaly and its related atmosphere and ocean processes regressed with the NAO+WP+ENSO index. We focus on the 3-7years band-pass time scale because the correlation with the El Niño in this time scale is the highest.

Figure 8 shows the correlation of the snow (upper) and surface air temperature (lower) in

(a), (b) December and (c), (d) January with the winter NAO+WP+ENSO index with the 3-7years band-pass filter. Positive correlation in the western Eurasian Continent is seen in figures 8a and 8c, and the negative correlation is seen in figures 8b and 8d in response to the snow anomaly. In addition, well correlated areas widen from December to January. These results signify that the negative NAO widens snow-covered area in the western Eurasian continent, and result in the cold anomaly there through the winter.

Figure 9 shows the correlation of the geopotential height at 500hPa (upper) and 850hPa (lower) in (a), (b) January and (c), (d) February. The cyclonic anomaly is seen over the western Eurasian continent in January, and the anticyclonic anomaly is seen over Tibetan plateau in January and February. This anticyclonic anomaly is located at the downstream of the cyclonic anomaly. Because the anticyclone over Tibetan plateau has the potential to intensify the cold air outbreak from Asia to the tropical zone, and to induce western wind burst on the western tropical Pacific, we examine the correlation of the meridional wind and zonal wind with the winter NAO+WP+ENSO index.

Figure 10 shows the latitude-height cross section of the meridional wind along the average from 110E° to 120E° (upper) and the longitude-height cross section of the zonal wind along the equator (lower) in (a) January, (b) (c) February and (d) March. The northern wind anomaly can be seen between equator and 10°N in the lower troposphere both in January and February, suggesting that the cold air outbreak is intensified by the anticyclonic anomaly over Tibetan plateau. In addition, the western wind anomaly can be seen in the zonal wind in February and March, which accord well with the northern with negative NAO. These processes starting from negative NAO can induce the occurrence of the El Niño from summer to winter.

5. Conclusions

We have newly demonstrated that positive (negative) phase of wintertime WP pattern, which brings warm (cold) anomaly to Japan along with East Asia, is related to the negative phase of NAO in the previous winter by statistical analyses. This year-to-year linkage may have a potential for long-term weather prediction. This study proposed two routes for this year-to-year linkage. One is the Arctic route and the other is the tropic route. The key factor for the Arctic route is the Arctic sea ice. The negative (positive) phase of the winter NAO weakens (strengthens) the poleward temperature advection by both the atmosphere and ocean. This weakened (strengthened) warm advection also speeds up (speed down) the springtime sea-ice reduction. This more (less) ice condition than normal persists until the season of the ice freezing in autumn. In winter, all the arctic is covered by sea ice regardless of the autumn ice area. The more the ice produces the more the heat releases to the atmosphere. This anomalous heat flux from the ocean to the atmosphere excites the Rossby wave propagation, which induce the cold advection to Japan. The influence of the NAO from this route is low-frequency, like decadal time-scale, variation. This is reasonable because sea ice and ocean have large heat capacity.

Another route is from the ENSO. This study found that negative winter NAO induces El Niño in the following winter. Because El Niño remotely excites the WP pattern, winter NAO can induce the WP pattern in the following winter. The time-scale of this NAO influence is 3-7 years, which accords well with the time scale of ENSO. The process from the winter negative NAO to El Niño is as follows. Anomalously wide snow cover in the western Eurasian Continent by the influence of the negative phase of the winter NAO, which brings about cold winter in the Europe, makes the air temperature in the region low. This negative heat release excites the cyclonic anomalous circulation over the temperature anomaly, and wave propagation excites the anticyclonic circulation over the Tibetan plateau. This anticyclonic circulation brings about the cold air outbreak from Asia to the western tropical Pacific Ocean, which intensifies the western wind burst on the western tropical Pacific Ocean. This western wind burst can excites El Niño in the following

summer to winter.

In consequence, both the long-term and short-term variations of the winter NAO act induce the WP in the following winter. Therefore, the phase of the NAO in the previous winter would be a predictor of the WP. We have proposed two processes for the connectivity of NAO and WP. Other hidden processes may influence the WP in the following winter. This must be done in future. To confirm the proposed processes, the usage of some Coupled Global Climate Model (CGCM) study is the next step.

Acknowledgments

I extend grateful thanks to Prof. Tachibana whose enormous support and insightful comments were invaluable during the course of my study. Also, I extend grateful thanks to Dr. Nakamura whose meticulous comments about the snow processes from the winter NAO to the following winter WP were an enormous help to me.

Members of climate and ecosystems dynamics laboratory and course of geosystem science in faculty of bioresources at Mie University assisted to this observation and provide some advices for my research. I would like to thank for them. In particular, laboratory's member always helped me in daily life so I enjoyed master's course for two years.

References

- Barnett, T. P., L. Dumenil, V. Schlese, E. Roeckner, and M. Latif 1989 : The effect of Eurasian snow cover on regional and global climate variations, *J. Atmos. Sci.*, **46**, 661–685.
- Clark, M. P., M. C. Serreze, and D. A. Robinson, Atmospheric controls on Eurasian snow extent, *Int. J. Climatol.* , **19**, 27–40, 1999.
- Honda, M., J. Inoue, and S. Yamane, 2009 : Influence of low Arctic sea-ice minima on anomalously cold Eurasian winters, *Geophys. Res. Lett.* **36**: L08707, doi: 10.1029 /2008GL037079.
- Horel, J.D., and J.M. Wallace, 1981 : Planetary-scale atmospheric phenomena associated with the Southern Oscillation. *Mon. Wea. Rev.*, **109**, 813-829.
- Hori, M. E. and T. Yasunari 2003: NAO impact towards the springtime snow disappearance in the western Eurasian continent, *Geophys. Res. Lett.*, **30(19)**, 1977, doi:10.1029/2003GL018103.
- Hori, M.E., et al., Recurrence of Intraseasonal Cold Air Outbreak during the 2009/2010 Winter in Japan and its Ties to the Atmospheric Condition over the Barents-Kara Sea, *SOLA*, 2011, Vol.7, **025-028**, doi:10.2151/sola.2011-007.
- Kalnay, E., et al. 1996: The NCEP/NCAR 40-year reanalysis project, *Bull. Am. Meteorol. Soc.*, **77**, 437–471.
- Kodera, K., 1998 : Consideration of the origin of the different midlatitude atmospheric responses among El Nino events. *J. Meteor. Soc. Japan*, **76**, 347-361.
- Mo, K. C., and R. E. Livezey, 1986: Tropical-extratropical geopotential height teleconnections during the Northern Hemisphere winter. *Mon. Wea. Rev.*, **114**, 2488-2515.
- Nakamura, T., Y. Tachibana, M. Honda, and S. Yamane, 2006 : Influence of the Northern Hemisphere annular mode on ENSO by modulating westerly wind bursts, *Geophys. Res. Lett.*, **33**, L07709, doi:10.1029/2005GL025432.
- Nakamura, T., Y. Tachibana, and H. Shimoda, 2007 : Importance of cold and dry surges in substantiating the NAM and ENSO relationship, *Geophys. Res. Lett.*, **34**, L22703, doi:10.1029/2007GL031220.

Ogi, M., Y. Tachibana, and K. Yamazaki, 2003 : Impact of the wintertime North Atlantic Oscillation (NAO) on the summertime atmospheric circulation, *Geophys.Res. Lett.* **30**: 1704, doi: 10.1029 /2003GL017280.

Rayner, N. A., D. E. Parker, E. B. Horton, C. K. Folland, L. V. Alexander, D. P. Rowell, E. C. Kent, and A. Kaplan, 2003: Global analyses of SST, sea ice and night marine air temperature since the late nineteenth century. *J. Geophys. Res.*, **108**, 4407, doi:10.1029/2002JD002670.

Rodwell, M. J., D. P. Rowell, and C. K. Folland, Oceanic forcing of the wintertime North Atlantic oscillation and European climate, *Nature*, **398**, **320–323**, 1999.

Takano, Y., Y. Tachibana, and K. Iwamoto 2008: Influence of large-scale atmospheric circulation and local sea surface temperature on convective activity over the Sea of Japan in December, *Sci. Online Lett. Atmos.* **4**, **113–116**.

Wallace, J. M., and D. Gutzler , 1981 : Teleconnections in the geopotential height field during the Northern Hemisphere winter, *Mon. Weather Rev.*, **109**, **784– 812**.

Figure Captions

Fig1. The correlation maps of (a) the geopotential height at 500hPa and (b) the temperature at 1000hPa in December with WP index.

Fig2. The correlation map of the geopotential height at 500hPa in the previous December with the WP index.

Fig.3 The correlation map of the EOF analysis for the data which combined the NAO area in December with WP area in the following December.

Fig4. The correlation of the sea-ice in spring (left), summer (middle) and autumn (right) with the high (upper), middle (middle) and low (lower) frequency NAO+WP index. We define that spring is March, April and May, summer is June, July and August and autumn is September, October and November.

Fig5. The correlation map of the SST in the following December with the NAO+WP index.

Fig6. The time-longitude cross section of SST correlations with the time filtered NAO+WP index. High-pass filters less than a) 3years, b) 5years, c) 7years and d) band-pass between 3 and 7years.

Fig7. The correlation map of the EOF analysis for the data which coupled the three area; the NAO area in December, WP area and El Niño/La Niña area in the following December.

Fig8. The correlation of the snow (upper) and surface air temperature (lower) in (a), (b) December and (b), (d) January with the NAO+WP+ENSOIndex of the 3-7 years bandpass.

Fig9. The correlation of the 500hPa (upper) and 850hPa (lower) of the geopotential height in (a), (b) January and (b), (d) February with the NAO+WP+ENSO index of the 3-7 years bandpass.

Fig10. The correlation of the meridional wind (upper) and zonal wind (lower) in (a) January, (b) (c) February and (d) March with the NAO+WP+ENSO index of the 3-7 years bandpass.

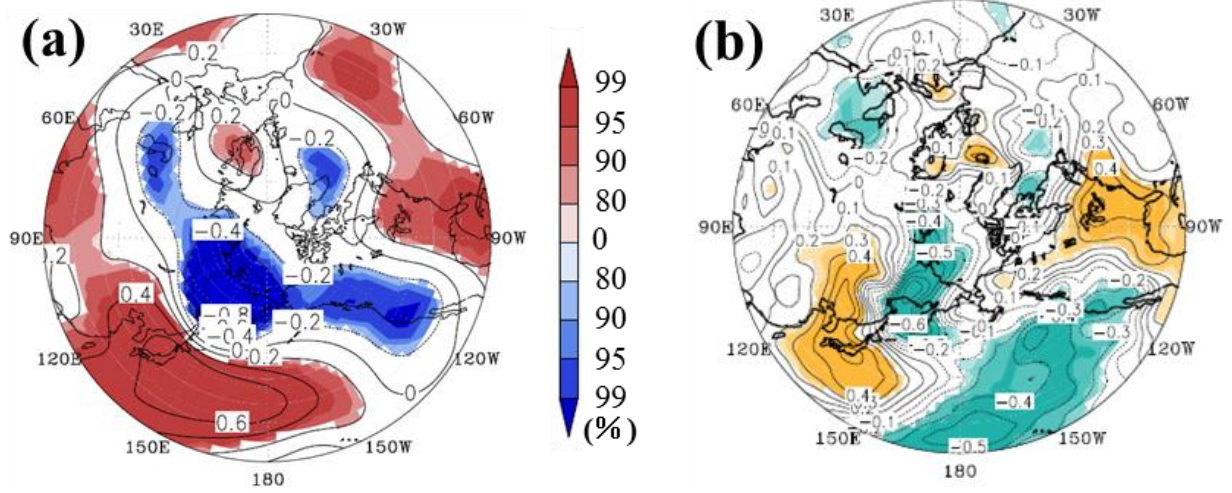


Fig1. The correlation maps of (a) the geopotential height at 500hPa and (b) the temperature at 1000hPa in December with WP index.

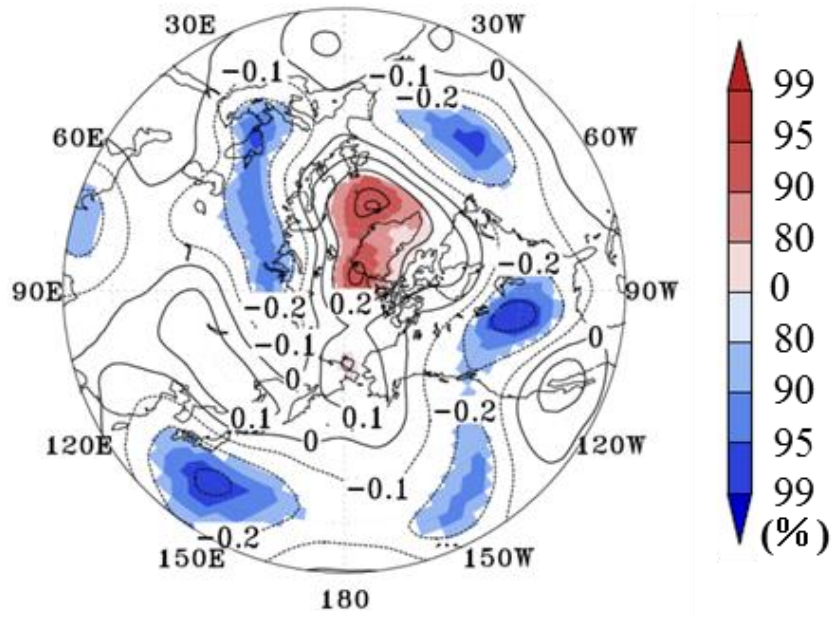


Fig2. The correlation map of the geopotential height at 500hPa in the previous December with the WP index.

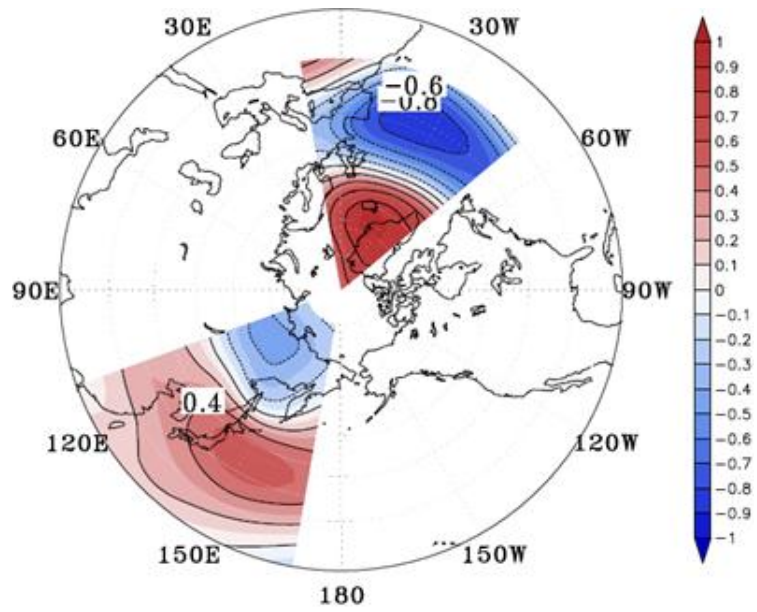


Fig.3 The correlation map of the EOF analysis for the data which combined the NAO area in December with WP area in the following December.

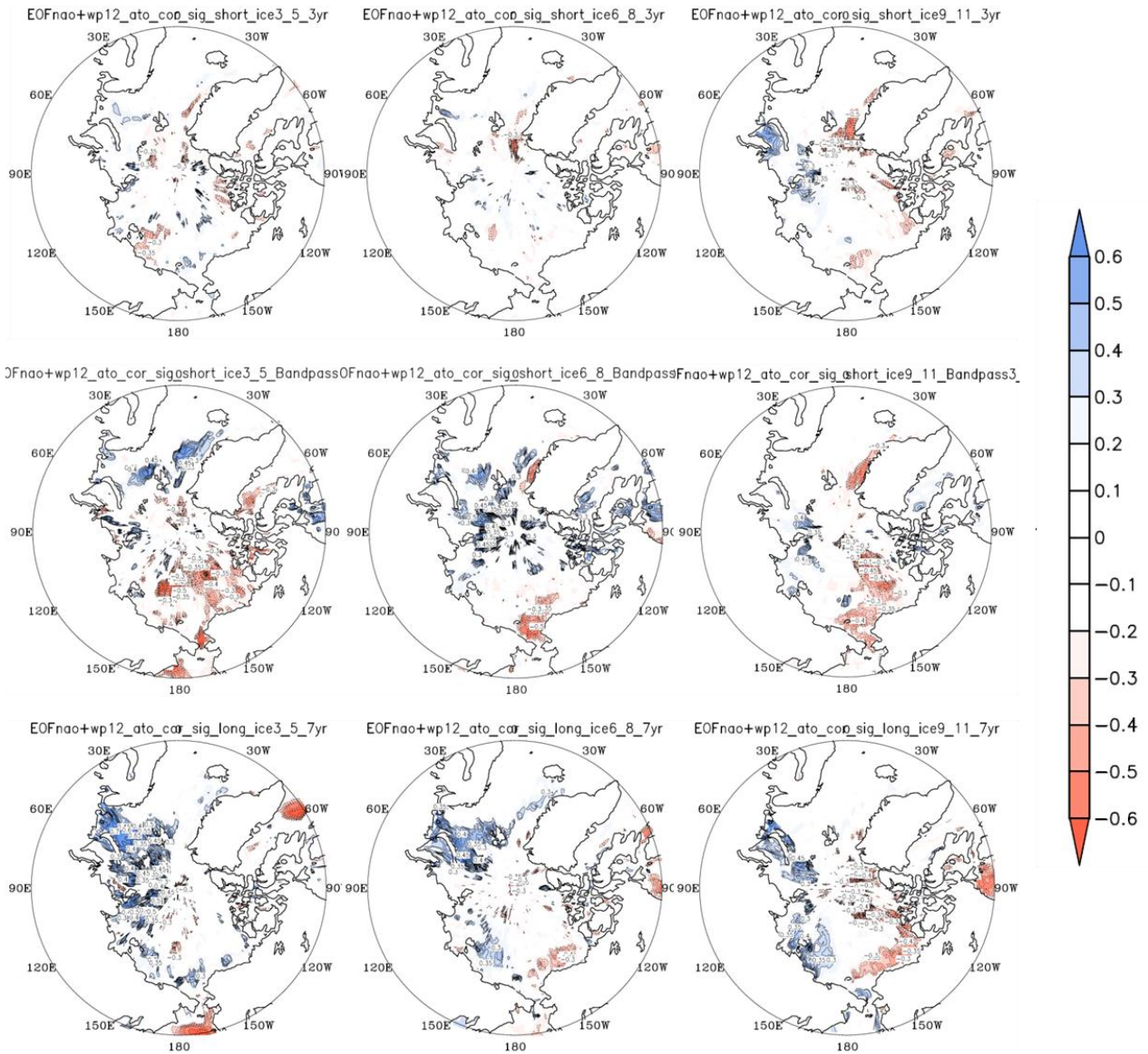


Fig4. The correlation of the sea-ice in spring (left), summer (middle) and autumn (right) with the high (upper), middle (middle) and low (lower) frequency NAO+WP index.

We define that spring is March, April and May, summer is June, July and August and autumn is September, October and November.

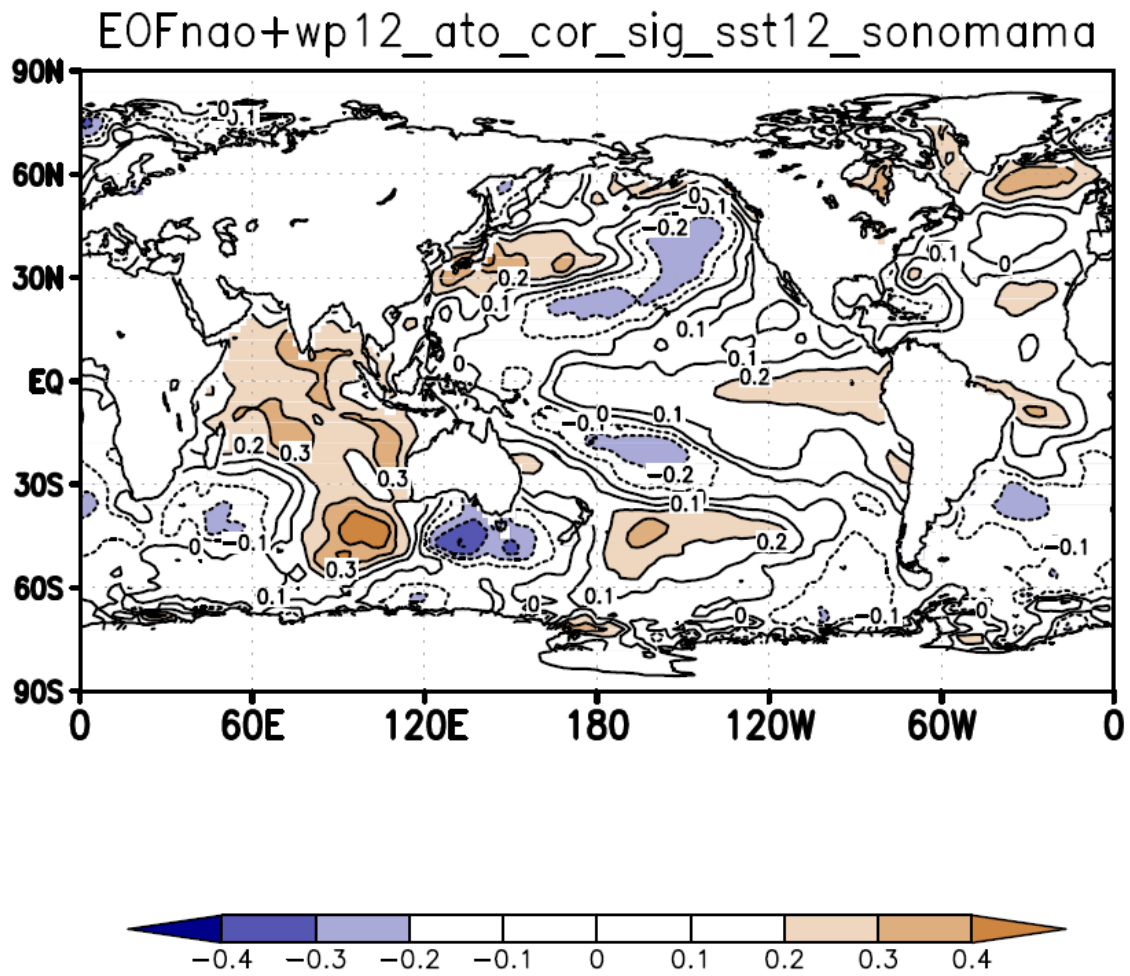


Fig5. The correlation map of the SST in the following December with the NAO+WP index.

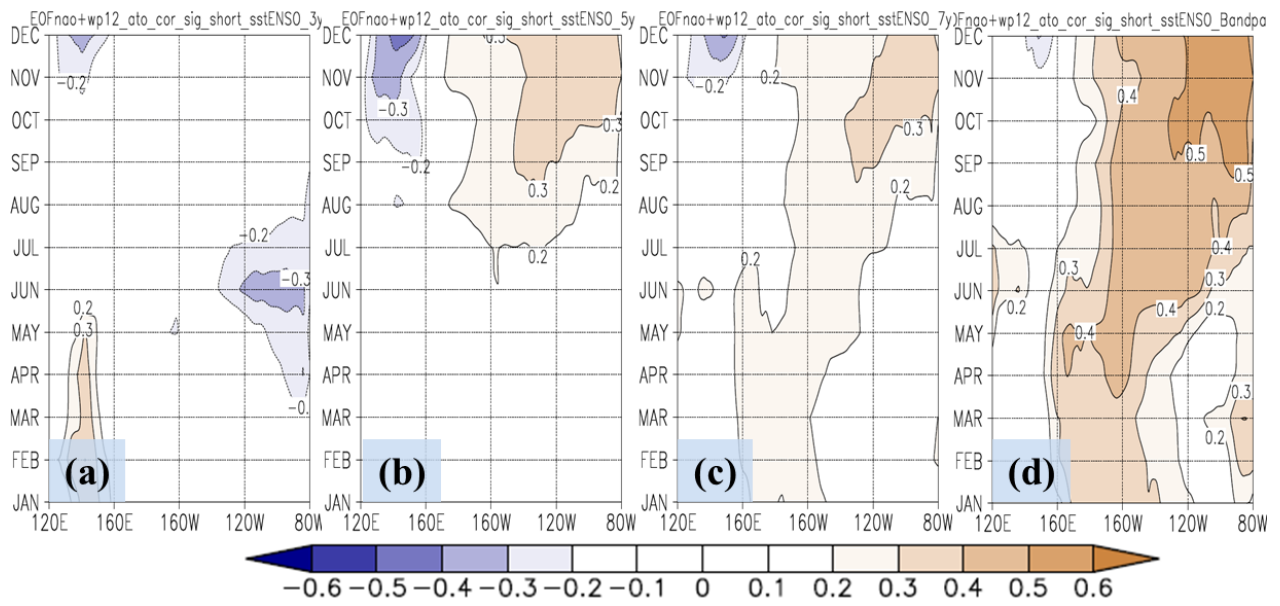


Fig6. The time-longitude cross section of SST correlations with the time filtered NAO+WP index. High-pass filters less than a) 3years, b) 5years, c) 7years and d) band-pass between 3 and 7years.

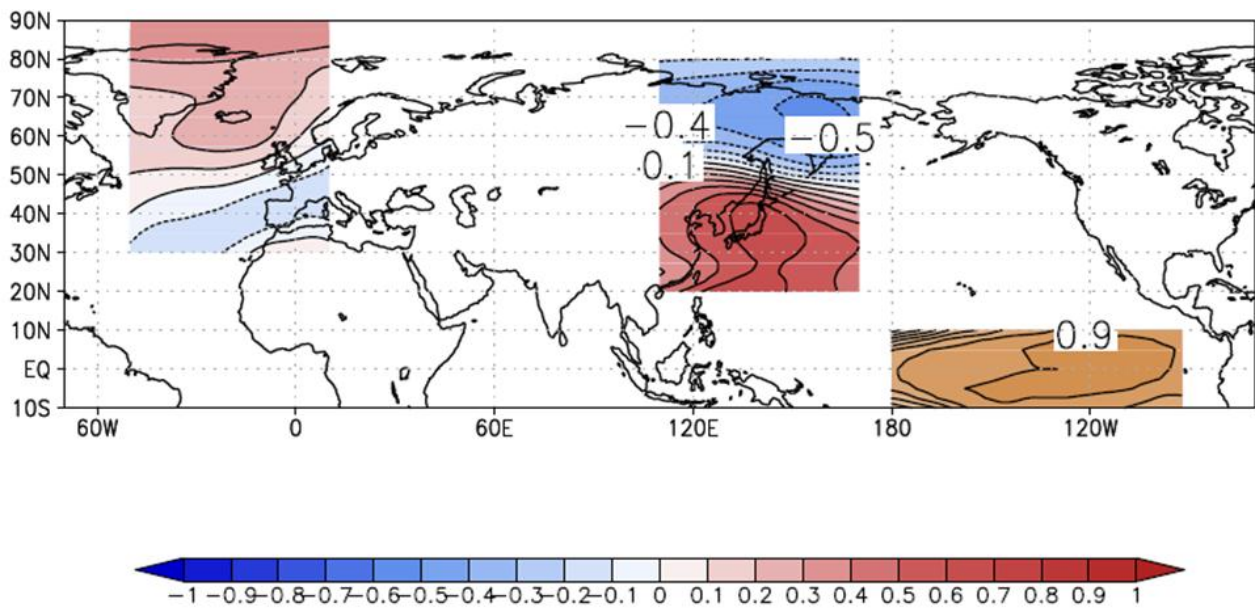


Fig7. The correlation map of the EOF analysis for the data which coupled the three area; the NAO area in December, WP area and El Niño/La Niña area in the following December.

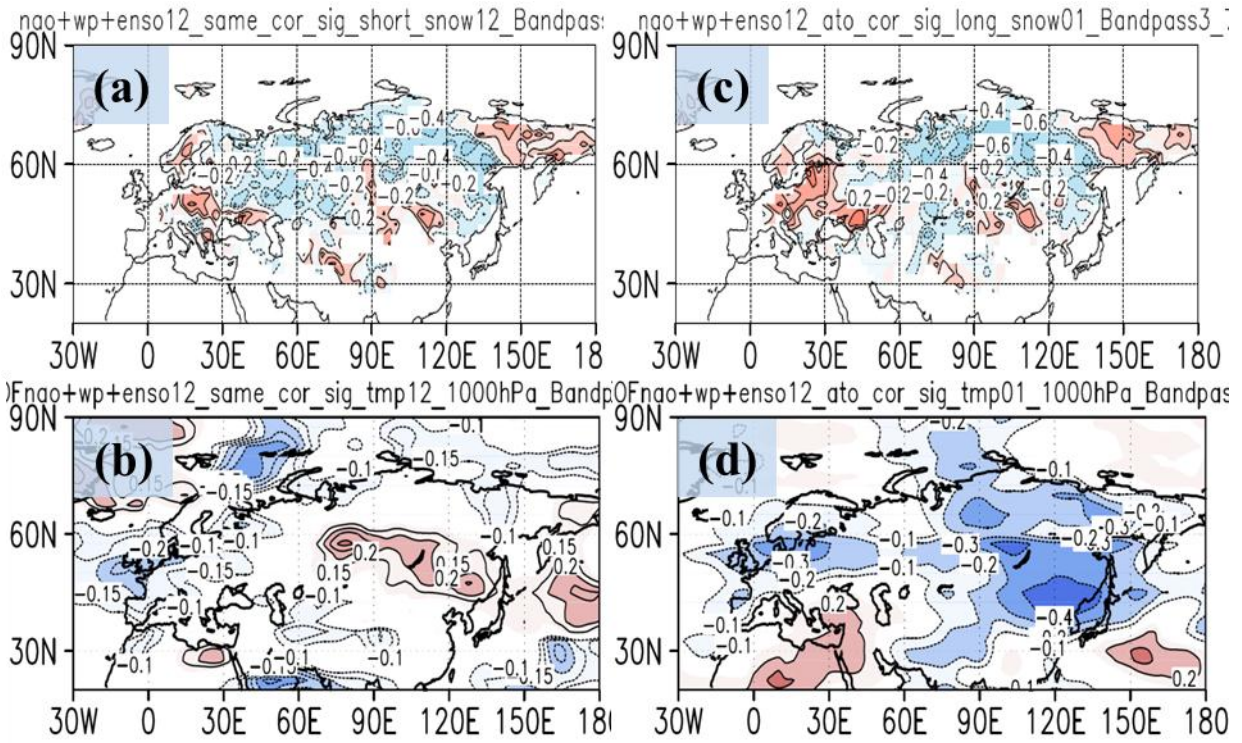


Fig8. The correlation of the snow (upper) and surface air temperature (lower) in (a), (b) December and (c), (d) January with the NAO+WP+ENSO Index of the 3-7 years bandpass.

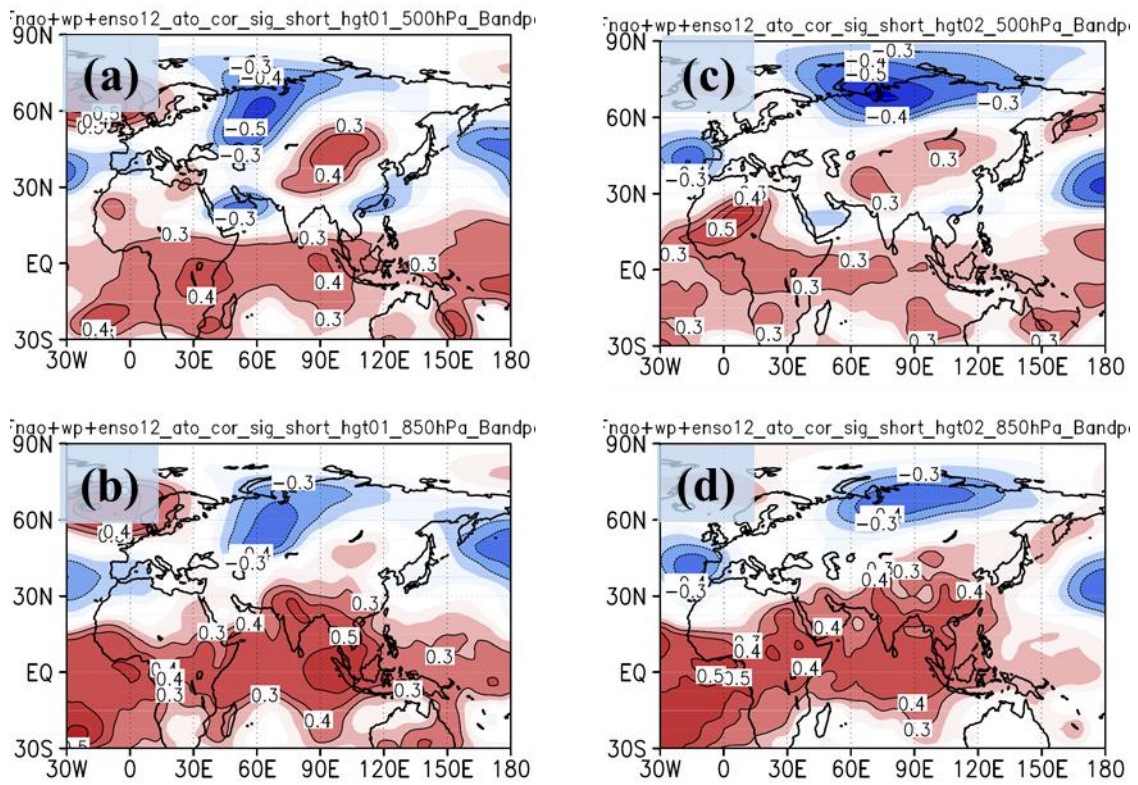


Fig9. The correlation of the 500hPa (upper) and 850hPa (lower) of the geopotential height in (a), (b) January and (b), (d) February with the NAO+WP+ENSO index of the 3-7 years bandpass.

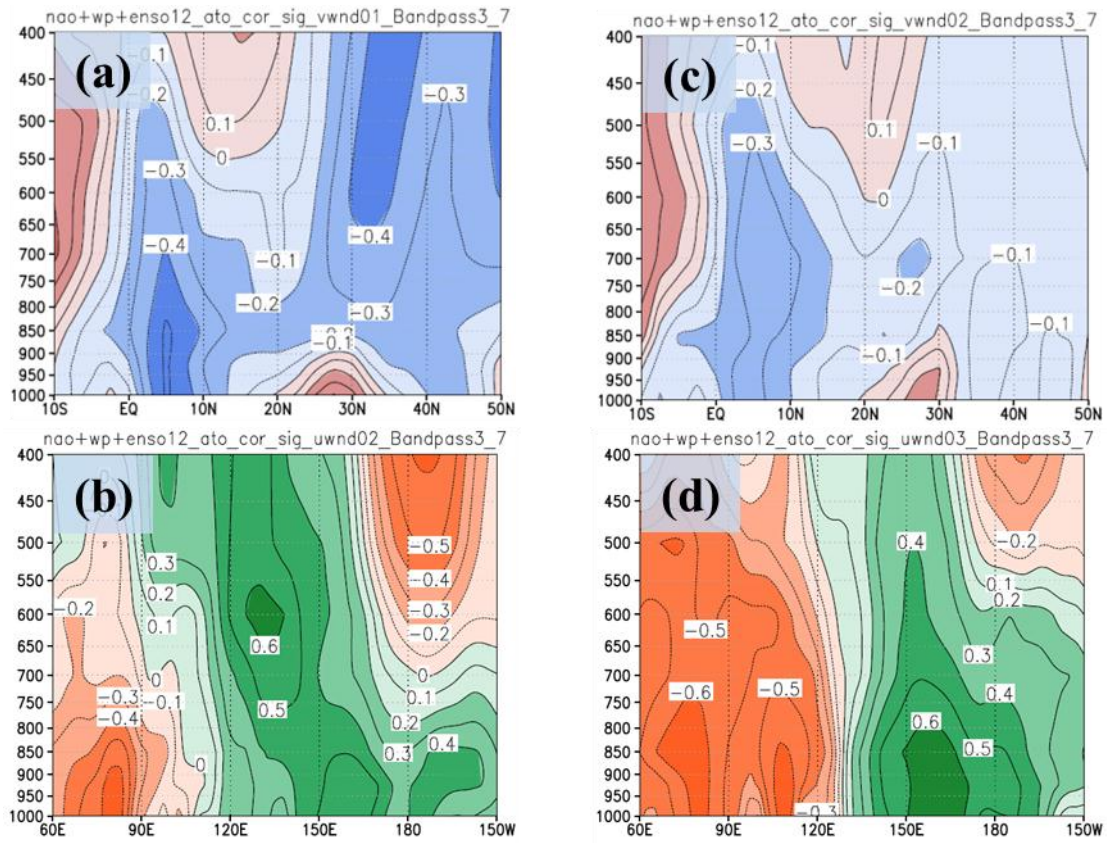


Fig10. The correlation of the meridional wind (upper) and zonal wind (lower) in (a) January, (b) (c) February and (d) March with the NAO+WP+ENSO index of the 3-7 years bandpass.